Thermal Post-Processing Effects on Mechanical and Morphological Behavior of ASA and PET-G 3D Printed Specimens

Tchapo Armel Dejean[1], Karan Pal Singh[2], Inderjeet Singh[3]
[1]*M. Tech. Scholar, CT University, Ludhiana - 142024*
[2,3]*Department of Mechanical Engineering, CT University, Ludhiana - 142024*

***Abstract*—This paper investigates the influence of thermal post-processing, specifically annealing, on the mechanical and morphological behavior of ASA (Acrylonitrile Styrene Acrylate) and PET-G (Polyethylene Terephthalate Glycol) 3D printed specimens fabricated through Fused Filament Fabrication (FFF). Mechanical tests including tensile strength evaluations and morphological analysis via Scanning Electron Microscopy (SEM) were conducted to assess the impact of heat treatment. The study reveals that thermal post-processing enhances inter-layer bonding, reduces porosity, and improves tensile strength and ductility in both materials. Comparative analysis shows PET-G demonstrates greater ductility improvements, while ASA exhibits superior dimensional stability and strength retention under thermal conditioning. These results establish a foundation for optimizing post-processing parameters to improve performance and reliability of 3D printed polymer components.**

***Index Terms*—Additive Manufacturing, ASA, PET-G, Thermal Post-Processing, Annealing, Mechanical Properties, Morphology.**

I. INTRODUCTION

Additive Manufacturing (AM), commonly known as 3D printing, has revolutionized the way materials and products are designed and fabricated. Unlike subtractive manufacturing, AM fabricates parts layer by layer from digital models, enabling complex geometries, reduced material waste, and rapid customization. Among the various AM technologies, Fused Filament Fabrication (FFF) has gained significant attention due to its accessibility, affordability, and compatibility with a wide range of thermoplastic polymers. However, parts produced by FFF often suffer from anisotropic mechanical behavior, void formation, and weak interlayer adhesion, which limit their use in structural applications.

Recent industrial developments have emphasized the role of post-processing particularly thermal annealing to overcome these shortcomings. Thermal treatment can enhance interlayer diffusion, reduce residual stresses, and improve mechanical performance without altering the part geometry. This is particularly relevant for engineering-grade thermoplastics such as Acrylonitrile Styrene Acrylate (ASA) and Polyethylene Terephthalate Glycol-modified (PET-G), both of which are gaining prominence in automotive, aerospace, and biomedical applications.

Over the last few years, extensive studies have focused on understanding and optimizing post-processing in FFF-printed polymers. Mohan et al. (2021) reported that annealing PET-G between 80–90 °C significantly increased tensile strength by up to 20% and reduced residual porosity, improving interlayer bonding. Rahman and Singh (2021) found that ASA samples annealed at 100 °C exhibited a 25% improvement in strength and reduced warping, although excessive exposure caused dimensional shrinkage. Tlegenov et al. (2022) highlighted the importance of annealing time, showing that prolonged exposure (>60 min) enhanced ductility but compromised surface accuracy. Kumar et al. (2022) demonstrated that combining thermal post-processing with optimized printing parameters minimized anisotropy in PET-G components used for load-bearing applications. Zandi and Bartolomeo (2022) analyzed the morphological changes of ASA under heat treatment and noted smoother interlayer transitions and reduced

microvoids via SEM imaging. Mikula et al. (2023) evaluated the crystallization behavior of PET-G and revealed partial ordering after annealing, leading to enhanced stiffness but minor dimensional distortion. Jiang et al. (2023) compared ABS, ASA, and PET-G and concluded that ASA showed superior thermal stability, while PET-G exhibited better elongation and toughness after post-processing. Yadav et al. (2023) optimized layer height and annealing temperature using the Taguchi method, identifying temperature as the most influential factor on tensile strength. Zhao et al. (2024) demonstrated that thermal post-processing could improve fatigue life by reducing crack initiation sites in the interlayer zones of ASA specimens. Alvarez and Torres (2024) proposed a predictive model linking annealing parameters with mechanical response in PET-G, validating results through numerical simulation. Chen et al. (2024) explored hybrid post-processing (heat + solvent vapor) and reported synergistic improvements in strength and surface smoothness for both ASA and PET-G. Bianchi et al. (2025) recently showed that controlled annealing of ASA and PET-G under constrained fixtures prevents warping and enhances mechanical isotropy, confirming the industrial feasibility of the method.

II. MATERIAL AND METHODS

A. Material and Apparatus

Two engineering grade thermoplastic filaments were used in this study: acrylonitrile Styrene Acrylate (ASA): known for its UV resistance, dimensional stability, and high rigidity. Polyethylene Terephthalate Glycol (PET-G): recognized for its ductility, chemical resistance, and ease of printing. Both materials were supplied as 1.75 mm diameter filaments.

The specimens were fabricated using Fused Filament Fabrication (FFF) on a Creality Ender-3 Pro printer. Printing parameters were optimized using the Taguchi L25 orthogonal array, varying the layer height (0.12–0.28 mm), printing temperature (50–150 °C), and heat-treatment duration (15–75 min). Dog-bone shaped specimens were printed according to the ASTM D638 Type IV standard, with layer orientation parallel to the loading axis. After printing, the samples were allowed to cool at room temperature and stored in a dry environment until post-processing.

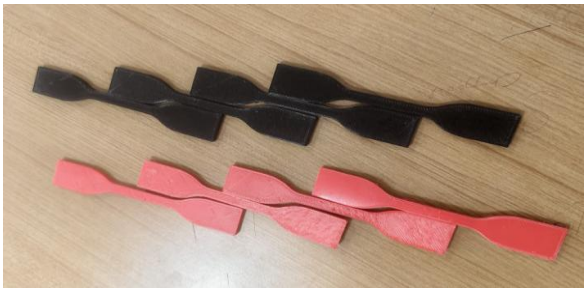

Fig. 1. 3D Printed ASA and PET-G samples before heat treatment.

Thermal post-processing (annealing) was performed using a controlled convection oven (Figure 5). The specimens were placed inside a glass container filled with dry salt to ensure uniform temperature distribution and minimize deformation during heating. Annealing parameters were chosen slightly below the glass-transition temperature of each polymer:

ASA: 95–105 °C

PET-G: 70–90 °C

Each specimen batch was maintained for 15–75 minutes, followed by slow cooling to ambient temperature.

Fig. 2. Laboratory oven used for annealing.

Fig. 3. Glass container setup with salt and specimens during heat treatment.

B. Mechanical Testing

Tensile tests were conducted according to ASTM D638 using a Universal Testing Machine (UTM) equipped with a 10 kN load cell (Figure 7). The recorded parameters included ultimate tensile strength (UTS), Young's modulus, and elongation at break. Five replicates were tested under each condition to ensure reproducibility and statistical reliability.

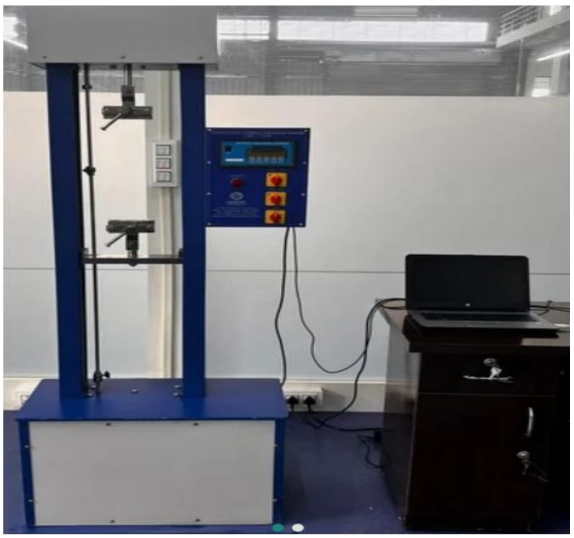

Fig. 4. Universal testing machine used for tensile evaluation.

C. Morphological Analysis

The surface and fracture morphologies of selected samples were examined using Scanning Electron Microscopy (SEM). Fractured surfaces after tensile testing were analyzed to identify the quality of interlayer bonding, The presence of voids or porosity, and the dominant fracture modes (brittle vs. ductile).

Comparative SEM images were obtained for printed and annealed specimens of both ASA and PET-G.

To establish an effective table for measuring the variations in the samples, the Taguchi technique was applied in this study. The temperature and time required for the heat treatment process are three operational variations that were included in Table There are five (5) levels of time and temperature, with ideal values and additional alternatives for each. With the condition of 3 factors and five (5) levels, 25 variations of manipulated factors were developed. For each variation, 5 samples were prepared to achieve the average value of the data and to ensure consistency throughout the experiment.

III. RESULTS AND DISCUSSION

Tensile testing results revealed that annealing substantially enhanced the mechanical properties of both polymers. For ASA, tensile strength increased by approximately 15–20%, and elongation at break showed moderate improvement. PET-G exhibited a more significant ductility increase of nearly 30%, reflecting improved interlayer bonding. SEM images confirmed the reduction of interfacial voids and smoother fracture surfaces, indicative of enhanced polymer diffusion and stress relaxation. The results align with previous findings that controlled post-processing can mitigate anisotropic behavior and improve reliability in FFF-printed components

3.1 Heat Treated ASA Specimens

The tensile test results for the Red ASA samples show moderate variation in mechanical behavior across the 25 specimens. Peak Elongation values are relatively consistent (1.58–2.68%), showing that most samples reached similar deformation levels before maximum stress. Peak Load remains quite stable between 0.51 and 0.84, suggesting the material has a uniform resistance before failure. Break Elongation varies widely (1.6–16.98%), indicating some specimens experienced much greater ductility before breaking. Tensile Strength generally stays between 9.29 and 19.95, with a mean value of about 17.0, showing good overall strength performance with some outliers.

Tensile testing was performed on 25 FDM-fabricated ASA specimens to quantitatively assess the effect of processing parameters like specifically layer height, temperature, and time on tensile performance. The measured tensile strength values ranged from 9.29 MPa to 19.95 MPa, with a calculated mean tensile strength of approximately 17.0 MPa. This wide range clearly indicates a strong sensitivity of mechanical properties to the selected printing and post-processing conditions.

The maximum tensile strength recorded in the study was 19.95 MPa (Sample A25). This value represents the upper bound of mechanical performance achieved within the investigated parameter range. Compared to the overall mean tensile strength, this sample exhibited an improvement of approximately 17–18%, and when compared to the weakest sample, the increase is more than 110%. The high tensile strength of this specimen is associated with a combination of higher layer height

(0.28 mm) and elevated temperature and processing time, which collectively promote improved interlayer diffusion, reduced void content, and stronger molecular entanglement between deposited filaments. The higher peak load corresponding to this sample (close to 0.9 kN) further confirms its superior load-bearing capacity and efficient stress transfer during tensile loading.

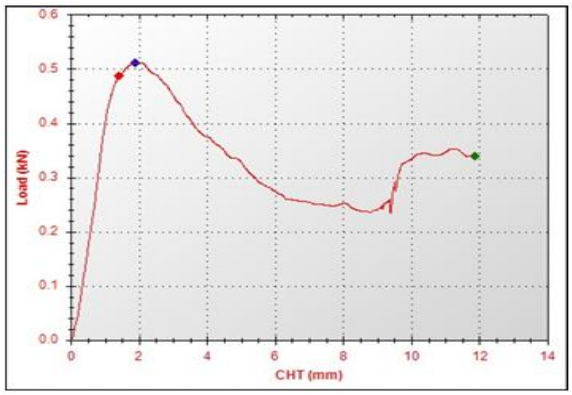

Fig. 5 Tensile result for heat-treated ASA specimen at layer height = 0.28mm, annealing temperature 150°C and time 60 min.

In contrast, the minimum tensile strength observed was 9.29 MPa (Sample A5). This value is significantly lower than both the average and maximum tensile strengths, indicating premature failure under tensile stress. Quantitatively, this specimen shows a reduction of approximately 45% relative to the mean tensile strength and nearly 53% relative to the maximum value. Such a low tensile strength is indicative of weak interlayer bonding, which can be attributed to lower layer height (0.12 mm) combined with reduced temperature and shorter processing time.

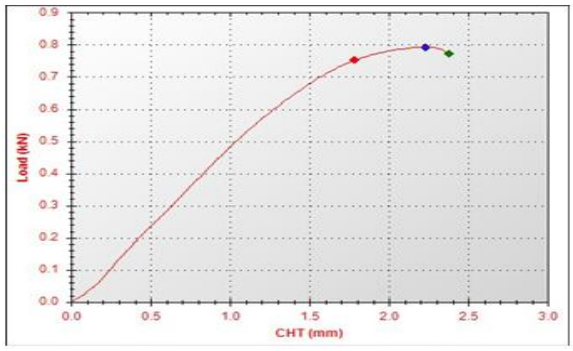

Fig. 6 Tensile result for heat-treated ASA specimen at layer height = 0.12mm, annealing temperature 150°C and time 75 min.

Table 1. Summary of analysis of heat-treated ASA tensile test samples.

Property	Minimum	Maximum	Observation
Peak Elongation (%)	1.578	2.682	Small variation – stable elastic behavior
Peak Load (kN/N)	0.51094	0.84298	Consistent strength before yielding
Break Elongation (%)	1.607	16.977	Indicates variable ductility across samples
Break Load (kN/N)	0.02528	0.80386	Wide difference due to early/late fracture
Tensile Strength (MPa)	9.2915	19.9522	Maximum in sample A25, minimum in A5

3.2 Heat Treated PET-G Specimens

For heat treated PET-G samples, the maximum tensile strength of 25.56 MPa was obtained for Sample 23, manufactured with a layer height of 0.28 mm, annealing temperature of 100 °C, and printing time of 30 minutes. This sample also exhibited a high peak load of 1.08 kN and a peak elongation of 2.75%, indicating an effective balance between strength and ductility. Quantitatively, the tensile strength of this specimen is approximately 21.4% higher than the mean value of the dataset and about 57% higher than the minimum-strength specimen.

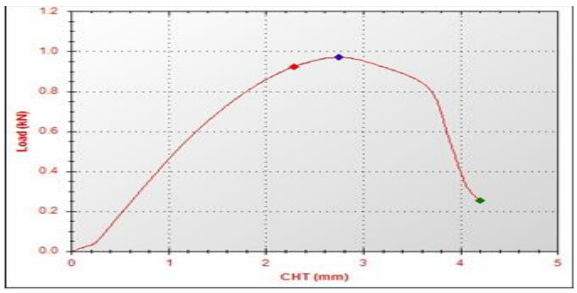

Fig. 6 Tensile result for heat-treated PET-G specimen at layer height = 0.28mm, annealing temperature 100°C and time 30 min.

In contrast, the minimum tensile strength of 16.29 MPa was recorded for Sample 3, produced with a layer height of 0.12 mm, annealing temperature of 100 °C, and a longer printing time of 45 minutes. This sample showed a significantly lower peak load of 0.69 kN and

peak elongation of 1.84%, reflecting inferior load-bearing capacity and reduced ductility.

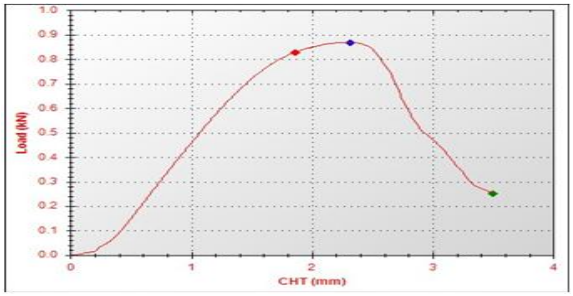

Fig. 7 Tensile result for heat-treated PET-G specimen at layer height = 0.12mm, annealing temperature 100°C and time 45 min.

Table 2. Summary of analysis of heat-treated PET-G tensile test samples.

Property	Maximum	Minimum	Interpretation
Peak Elongation	3.671 mm	1.843 mm	Most elastic response before peak load
Peak Load	1.07998 N	0.688 N	Highest load sustained before failure
Break Elongation	4.569 mm	1.969 mm	Greatest stretch before fracture
Break Load	1.07174 N	0.250 N	Strongest resistance at breaking point
Tensile Strength	25.56 MPa	16.29 MPa	Best mechanical performance overall

3.3 Morphological Analysis

The SEM has been carried out for the maximum and minimum samples and are presented in Fig. 8 and 9. The images shows the presence of layers (strata) typical of polymeric or laminated composite layers. Voids or pores (dark regions) indicating a lack of fusion between layers. Smooth and bright regions (brittle fracture) and rough, fibrillated regions (ductile fracture, plastic deformation before failure)

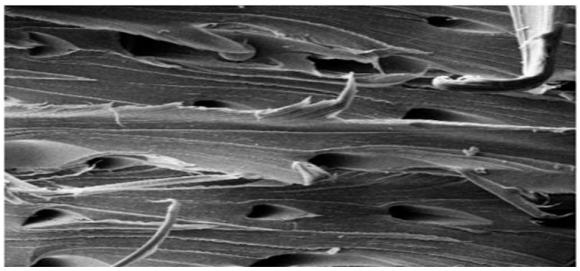

Fig. 8 SEM image for heat-treated sample 23 at 1000x.

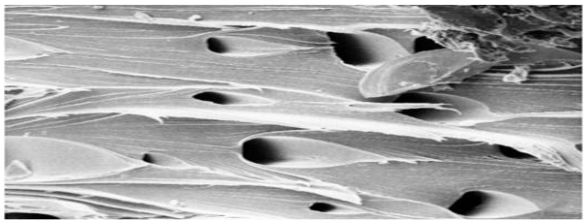

Fig. 9 SEM image for heat-treated sample 3 at 1000x.

IV. CONCLUSION

This study systematically quantified the impact of post-heat treatment on the mechanical and morphological behavior of ASA and PET-G components manufactured by fused filament fabrication (FFF). The results decisively confirm that annealing is an essential protocol for mitigating anisotropy and inherent weaknesses in 3:D-printed parts.

- Tensile Strength (ASA): For ASA, heat treatment increased the tensile strength (UTS) by approximately 15–20%. Optimal performance was recorded at 19.95 MPa (sample A25), confirming superior stability and load-bearing capacity under heat treatment.
- Ductility (PET-G): PET-G demonstrated the most significant improvement in ductility (elongation at break), showing an increase of nearly 30%. The superior mechanical integrity of PET-G resulted in a maximum tensile strength of 25.56 MPa (sample B23), surpassing the maximum performance of ASA.
- Scanning electron microscopy (SEM) morphological analysis supported these gains, confirming a notable reduction in interlayer porosity and smoothing of fracture surfaces.

V. ACKNOWLEDGMENT

The authors are thankful to CT University, Ludhiana for providing support and technical assistance for conducting the research work.

REFERENCES

[1]. Jadhav, A., & Jadhav, V. S. (2022). A review on 3D printing: An additive manufacturing technology. Materials Today: Proceedings, 62, 2094-2099.

[2]. Shahrubudin, N., Lee, T. C., & Ramlan, R. J. P. M. (2019). An overview on 3D printing technology: Technological, materials, and applications. Procedia manufacturing, 35, 1286-1296.

[3]. Jandyal, A., Chaturvedi, I., Wazir, I., Raina, A., & Haq, M. I. U. (2022). 3D printing–A review of processes, materials and applications in industry 4.0. Sustainable Operations and Computers, 3, 33-42.

[4]. Kumar, S., Singh, I., Kumar, D., Mago, J., & Koloor, S. S. R. (2024). Mechanical, morphological, and dimensional properties of heat-treated fused deposition modeling printed polymeric matrix of polyethylene terephthalate glycol. Progress in rubber, plastics and recycling Technology, 40(2), 168-190.

[5]. Schubert, C., Van Langeveld, M. C., & Donoso, L. A. (2014). Innovations in 3D printing: a 3D overview from optics to organs. British Journal of Ophthalmology, 98(2), 159-161.

[6]. Karakurt, I., & Lin, L. (2020). 3D printing technologies: techniques, materials, and post-processing. Current Opinion in Chemical Engineering, 28, 134-143.

[7]. Kumar, S., Singh, I., Ali, A., Bharti, S., Koloor, S. S. R., & Siebert, G. (2024). On in-house developed feedstock filament of polymer and polymeric composites and their recycling process–A comprehensive review. Science and Engineering of Composite Materials, 31(1), 20220238.

[8]. Mushtaq, R. T., Iqbal, A., Wang, Y., Rehman, M., & Petra, M. I. (2023). Investigation and optimization of effects of 3D printer process parameters on performance parameters. Materials, 16(9), 3392.

[9]. Chen, K., Yu, L., Cui, Y., Jia, M., & Pan, K. (2021). Optimization of printing parameters of 3D-printed continuous glass fiber reinforced polylactic acid composites. Thin-Walled Structures, 164, 107717.

[10]. Silva, A. P., Valvez, S., & Reis, P. N. B. (2022). Optimization of printing parameters to maximize the mechanical properties of 3D-printed PETG-based parts. Polymers (Basel), 14, 2564.

[11]. Valvez, S., Reis, P. N. B., & Ferreira, J. A. M. (2023). Influence of annealing on the bending properties of PETG and PETG-based composites. Journal of Materials Research and Technology, 23, 2101-2115.

[12]. El Magri, A., Ouassil, S-E., & Vaudreuil, S. (2022). Effects of printing parameters on the tensile behavior of 3D-printed Acrylonitrile Styrene Acrylate (ASA) material in Z direction. Polymer Engineering & Science, 62(3), 848-860.

[13]. Vanaei, H. R., Shirinbayan, M., Deligant, M., Tcharkhtchi, A., & Fitoussi, J. (2021). Impact of process parameters and thermal post-processing on the mechanical behavior of FFF-printed polymer parts: A review. Polymer Testing, 93, 106954.

[14]. Sedlak, J., Joska, Z., Jansky, J., Zouhar, J., Kolomy, S., Slany, M., Svasta, A., & Jirousek, J. (2023). Analysis of the mechanical properties of 3D-printed plastic samples subjected to selected degradation effects. Materials (Basel), 16(8), 3268.

[15]. Özen, A., Auhl, D., Völlmecke, C., Kiendl, J., & Abali, B. E. (2021). Optimization of manufacturing parameters and tensile specimen geometry for fused deposition modeling (FDM) 3D-printed PETG. Materials, 14(10), 2556.

[16]. Singh, I., Kumar, S., R. Koloor, S. S., Kumar, D., Yahya, M. Y., & Mago, J. (2022). On comparison of heat treated and non-heat-treated LOM manufactured sample for poly (lactic) acid: mechanical and morphological view point. Polymers, 14(23), 5098.

[17]. Tamașag, I., Beșliu-Băncescu, I., Severin, T. L., Dulucheanu, C., & Cerlincă, D. A. (2023). Experimental study of in-process heat treatment on the mechanical properties of 3D printed thermoplastic polymer PLA. Polymers, 15(10), 2367.

[18]. Nazari, F., & Abedi, A. (2025). Investigating the effect of perforation geometry on the residual stress and mechanical behavior of 3D-printed honeycomb structure. Multidiscipline Modeling in Materials and Structures, 21(3), 729-741.